Published in final edited form as:
Chembiochem. 2008 June 16; 9(9): 1487–1492. doi:10.1002/cbic.200800005.

Arginine Dynamics in a Membrane-Bound Cationic Beta-Hairpin Peptide from Solid-State NMR

Ming Tang[a], **Alan J. Waring**[b], and **Mei Hong**[a]

[a]Department of Chemistry, Iowa State University, Ames, IA 50011

[b]Department of Medicine, University of California at Los Angeles School of Medicine, Los Angeles, California 90095

Abstract

The site-specific motion of Arg residues in a membrane-bound disulfide-linked antimicrobial peptide, protegrin-1 (PG-1), is investigated using magic-angle spinning solid-state NMR, to better understand the membrane insertion and lipid interaction of this cationic membrane-disruptive peptide. C-H and N-H dipolar couplings and ^{13}C chemical shift anisotropies were measured in the anionic POPE/POPG membrane and found to be reduced from the rigid-limit values by varying extents, indicating the presence of segmental motion. An Arg residue at the β-turn region of the peptide shows much weaker spin interactions, indicating larger amplitudes of motion, than an Arg residue in the β-strand region of the peptide. This is consistent with the exposure of the β-turn to the membrane surface and the immersion of the β-strand in the hydrophobic middle of the membrane, and supports the previously proposed oligomerization of the peptide into β-barrels in the anionic membrane. ^{13}C T_2 and ^{1}H $T_{1\rho}$ relaxation times indicate that the β-turn backbone undergoes large-amplitude intermediate-timescale motion in the fluid phase of the membrane, causing significant line broadening and loss of spectral intensity. This study illustrates the strong correlation between the dynamics and the structure of membrane proteins and the capability of solid-state NMR spectroscopy for providing detailed information on site-specific dynamics in complex membrane protein assemblies.

Keywords

membrane protein dynamics; molecular dynamics; antimicrobial peptides; guanidinium-phosphate complexation; order parameters; solid-state NMR; arginine

Introduction

Molecular motion is common in membrane proteins and is often intimately related to the function and lipid-interaction of these molecules. Solid-state NMR (SSNMR) spectroscopy is a versatile tool to characterize molecular dynamics on a wide range of timescales (picoseconds to seconds) and to determine the amplitude of anisotropic motion. Large-amplitude segmental motion has been reported, for example, for a bacterial toxin that spontaneously inserts into the lipid membrane as a result of its intrinsic conformational plasticity [1], a lipidated Ras signaling protein [2], the catalytic domain of a membrane-bound enzyme [3], and the loops of the seven-transmembrane-helix protein rhodopsin [4]. In addition to internal segmental motion, whole-body reorientation has been discovered for many small membrane peptides of both β-sheet and α-helical secondary structures [5–7].

Corresponding author: Mei Hong, mhong@iastate.edu, Tel: (515) 294-3521, Fax: (515) 294-0105.

Protegrin-1 (PG-1) is a broad-spectrum antimicrobial peptide found in porcine leukocytes [8,9]. It is a β-hairpin molecule stabilized by two disulfide bonds and contains six Arg residues (RGGRLCYCRRRFCVCVGR). PG-1 achieves its antimicrobial function by forming non-selective pores in the microbial cell membrane that disrupt the membrane's barrier function [10,11]. Recently, the high-resolution oligomeric structure of PG-1 at the pores was determined using ^{1}H and ^{19}F spin diffusion NMR techniques [12]. The peptide was found to self-assemble into a transmembrane β-barrel in bacteria-mimetic anionic POPE/POPG membranes. ^{13}C-^{31}P distance constraints indicate that the Arg residues in these transmembrane β-barrels are complexed with lipid phosphates [13], suggesting that the charge neutralization by ion pairing reduces the free energy of peptide insertion into the hydrophobic part of the membrane, and the consequent tethering of lipid headgroups may be the cause for toroidal pore formation.

The experiments that yielded the equilibrium oligomeric structure of PG-1 and the toroidal pore morphology of the lipid membrane were carried out at low temperatures of about −40°C, in the gel phase of the membrane, to eliminate any motion that would average the distance-dependent dipolar couplings. On the other hand, PG-1 carries out its antimicrobial action in the liquid-crystalline (LC) phase of the membrane, where it is expected to be more mobile. How the dynamics of PG-1 and its Arg sidechains affect toroidal pore formation has not yet been studied. If Arg-phosphate complex formation is true, then the functional groups involved in the complex – the guanidinium ions, the lipid phosphates, and possibly water – should be less mobile than in their respective bulk environments. Thus, understanding Arg motion in PG-1 in the lipid membrane may provide additional insight into guanidinium-phosphate interaction. More generally, although the motion of long-chain amino acid residues has begun to be investigated in microcrystalline proteins [14–16], motion of the same residues in membrane proteins is still scarcely studied by NMR. Arg is particularly common in many medically important membrane peptides and proteins such as antimicrobial peptides (AMPs) [17], cell-penetrating peptides [18,19], and voltage-sensing domains of ion channels [20].

In this work we report the amplitudes of microsecond timescale motions of Arg and other residues in PG-1 bound to the POPE/POPG membrane. We found that an Arg in the β-strand part of the molecule, which is embedded in the hydrophobic interior of the membrane, is much less mobile than an Arg in the β-turn part of the molecule, which is exposed to the membrane surface. This is consistent with the oligomeric structure and lipid interaction of this antimicrobial peptide.

Results

We first characterized the dynamic structure of PG-1 in POPE/POPG bilayers by variable-temperature ^{13}C and ^{15}N CP-MAS experiments. A series of CP spectra were collected between 243 K and 308 K for PG-1 containing U-^{13}C, ^{15}N-labeled Arg_4, Leu_5, and Arg_{11}, and ^{15}N-labeled Phe_{12}. As shown in Figure 1, the Cα peaks of Arg_4 and Leu_5 are much sharper and higher than the Cα peak of Arg_{11}. At 295 K, the full widths at half-maximum (FWHM) of Arg_4 and Leu_5 Cα's are ~3 ppm, compared to 6 ppm for Arg_{11} Cα. As the temperature decreases, the Arg_{11} Cα intensity increases significantly. This suggests that in the liquid-crystalline phase of the membrane Arg_{11} backbone undergoes large-amplitude intermediate-timescale motion that becomes frozen in the gel phase of the membrane, while the Arg_4 and Leu_5 Cα sites are more rigid. In other words, the β-turn backbone is more mobile than the β-strand backbone. A similar trend is observed in the ^{15}N CP-MAS spectra (Figure 2). The backbone Nα peaks of Arg_4 and Leu_5 are sharp and well resolved, with FWHM of 2 – 3 ppm at 283 K, while the Arg_{11} Nα peak is broad and overlaps with Phe_{12} Nα, giving a FWHM of 9 ppm for the combined peak at 283 K. Only at 243 K do the Arg_{11}

Nα and Phe_{12} Nα peaks become resolved. We assigned the Nα peaks by ^{13}C-^{15}N 2D correlation experiments (data not shown) [21].

To distinguish the contribution of static structural heterogeneity versus dynamic disorder to the linewidths, we measured the ^{13}C T_2 of Arg_4 and Arg_{11} at two different temperatures, 283 K and 243 K, using the Hahn echo experiment. Table 1 shows the ^{13}C apparent linewidths, Δ*, read off from the CP spectra, and the ^{13}C homogeneous linewidths, Δ, obtained from the T_2 values according to $\Delta = 1/\pi T_2$. At 243 K, the homogeneous linewidths of Arg_4 and Arg_{11} are similar, indicating that motion is largely frozen. However, the apparent linewidth of Arg_{11} backbone Cα (604 Hz, or 6.0 ppm) is much larger than Arg_4 Cα (222 Hz, or 2.2 ppm), indicating that there is much larger conformational disorder at the β-turn backbone than at the β-strand. In comparison, the sidechains of Arg_4 and Arg_{11} at 243 K exhibit similar homogeneous linewidths as well as similar apparent linewidths, indicating that both the static and dynamic heterogeneities are comparable for the two sidechains. At 283 K, Arg_{11} Cα exhibits both larger Δ and larger Δ* than Arg_4 Cα, indicating that the β-turn backbone has greater dynamic as well as static disorder than the β-strand backbone. In contrast, the sidechain of Arg_{11} has narrower Δ and Δ* than the Arg_4 sidechain, indicating that Arg_{11} sidechain undergoes faster motions than Arg_4.

To obtain information on the motional amplitudes of the Arg sidechains, especially the guanidinium group, we measured the ^{13}C chemical shift anisotropy (CSA) of Cζ, the center of the guanidinium ion. We chose the intermediate temperature of 283 K for the CSA and the subsequent dipolar coupling experiments, since at this temperature the spectra have the best overall combination of resolution and sensitivity. The theoretical phase transition temperature of the POPE/POPG (3:1) membrane is 291 K, thus the spectra theoretically correspond to the gel-phase membrane, but the phase transition is likely broadened by the peptide. The peptide mobility closer to the physiological temperature may be extrapolated from the 283 K data and is expected to be higher, but the differences between residues should be similar. We used the 2D separation of undistorted powder patterns by effortless recoupling (SUPER) experiment [22] to recouple the CSA interaction and correlate it with the isotropic ^{13}C chemical shift. Figure 3 shows the 2D SUPER spectra and 1D cross sections of the model compound Fmoc-Arg(MTR)-OH, and Arg_4 and Arg_{11} in PG-1 bound to the POPE/POPG membrane. For the dry powder sample Fmoc-Arg(MTR)-OH, the Cζ cross section yielded a CSA anisotropy parameter δ, defined as the difference between the largest principal value δ_{zz} and the isotropic shift δ_{iso}, of 78 ppm. This CSA is the rigid-limit value, since C-H dipolar couplings of the sidechain carbons in this model compound have nearly rigid-limit values (Table 2). In comparison, PG-1 Arg_4 and Arg_{11} Cζ both give reduced CSA's: the Arg_4 Cζ δ is 47.3 ppm whereas the Arg_{11} Cζ CSA is much smaller, 10.3 ppm. These correspond to a motional scaling factor of 0.13 for Arg_{11} and 0.61 for Arg_4. Thus, the Arg_{11} sidechain has larger-amplitude motion than Arg_4. Since T_2 data indicate narrower homogeneous linewidths of Arg_{11} Cδ and Cζ than Arg_4, the Arg_{11} sidechain motion is both faster and larger in amplitude than the Arg_4 sidechain.

To obtain more quantitative information on the motional amplitude, we measured C-H and N-H dipolar couplings, whose tensor orientation and rigid-limit coupling strength are exactly known. The dipolar couplings were readily measured using the 2D dipolar-chemical shift correlation (DIPSHIFT) experiment to yield the bond order parameter, $S = \bar{\delta}/\delta$. Figure 4 shows representative DIPSHIFT curves of Arg_4 and Arg_{11} in POPE/POPG-bound PG-1. Cα-H represents the backbone, while Cδ-H_2, Nε-H and Nη-H_2 represent the sidechains. The order parameters are compiled in Table 2. Both the backbone Nα and Cα of Arg_4 and Leu_5 exhibit nearly rigid-limit couplings, with order parameters of 0.93–1.00. In contrast, the Arg_{11} Cα and Nα have significantly lower order parameters of 0.70. Thus, the β-strand backbone of the peptide is immobilized in the POPE/POPG membrane at this temperature,

while the Arg_{11} backbone retains significant local segmental motion. For resolved sites (Cδ, Nε, and Nη) in the sidechains, Arg_4 and Leu_5 also have stronger dipolar couplings than those of Arg_{11}, indicating that the β-strand sidechains have smaller amplitudes of motion, consistent with the variable-temperature spectra and the CSA results. Some ^{13}C sites in the sidechain, such as Arg Cβ, Cγ, Leu Cγ and Cδ, overlap with the lipid peaks, so we used a double-quantum (DQ) filtered DIPSHIFT experiment to suppress the lipid signals and measure the C-H couplings of these Arg sites [1]. Figure 5 shows representative 1D DQ spectra and DQ-DIPSHIFT dephasing curves of Arg_4 and Leu_5. Arg_{11} has prohibitively low sensitivity in the DQ-DIPSHIFT experiment due to unfavorable motional rates at this temperature and is thus not measured. Table 2 shows that in general, the sidechain order parameters decrease with increasing distance from the backbone. Arg_{11} at the β-turn, which is close to the membrane surface, has much higher amplitudes of motion, or much lower order parameters, than Arg_4 and Leu_5 in the β-strand part of the peptide, which is embedded in the membrane [12].

To obtain further information on the rates of motions of these residues, we measured the ^1H $T_{1\rho}$ relaxation times, listed in Table 3. Most sites in Arg_4, Leu_5 and Arg_{11} have similar ^1H $T_{1\rho}$ values (1.6 – 2.6 ms), except for Arg_{11} Hα, which has a much shorter $T_{1\rho}$ (0.83 ms) than Arg_4 Hα (2 ms). This is consistent with the ^{13}C T_2 data indicating more pronounced intermediate-timescale motion of the β-turn backbone compared to the β-strand backbone.

Discussion

The solid-state NMR data shown here indicate that the β-turn backbone undergoes large-amplitude segmental motion on the microsecond timescale, while the β-strand backbone is mostly immobilized in the POPE/POPG membrane in the liquid-crystalline phase. The latter is consistent with the previously reported immobilization of PG-1 strand residues in POPC/POPG membranes [23]. Concomitant with the backbone mobility difference, the sidechains also exhibit dynamic differences: Arg_{11} has much lower order parameters than Arg_4 (Table 2), indicating large motional amplitudes. Both membrane-associated Arg's are much more mobile than the crystalline compound Arg · HCl.

The dynamic difference between Arg_4 and Arg_{11} can be understood in terms of the self-assembly of PG-1 and the peptide-lipid interactions. The β-strands containing Arg_4 and Leu_5 are involved in intermolecular association with other PG-1 molecules through N–H···O=C hydrogen bonds to form β-barrels [12,24], thus these residues should experience hindered motion. The strand aggregation is important to PG-1 antimicrobial activity. Mutation of Val_{14} to *N*-methyl-Val, which disrupted hydrogen bonding of the Val_{14} backbone to its intermolecular partner, resulted in much lower antimicrobial activity [25]. In contrast, the β-turn Arg_{11} is not involved in intermolecular hydrogen bonding and is located near the membrane surface, thus has more motional freedom.

A second contributing factor to the different sidechain dynamics of Arg_{11} and Arg_4 may be the guanidinium-phosphate interaction. ^{13}C-^{31}P distance data indicated that both sidechains lie within hydrogen-bonding distance to lipid phosphates [13]. However, while the Arg_4 guanidinium group interacts with the phosphate groups that have moved to the middle of the membrane as part of the toroidal pore, the Arg_{11} guanidinium ion interacts with phosphates at the membrane surface with much higher mobility. Thus, the motional restriction caused by the lipid phosphate groups is more severe for Arg_4 than for Arg_{11}. We note that at the temperature of 283 K where most dynamics data were obtained, the lipid molecules are much more mobile than at ~230 K where the ^{13}C-^{31}P distances were measured. Thus, the guanidinium-phosphate association at 283 K is likely to be transient rather than permanent.

The high mobility of the β-hairpin tip of PG-1 dovetails the observation of an analogous β-hairpin antimicrobial peptide, TP-I [26]. There, G10 at the β-turn exhibited an order of magnitude shorter ^{1}H $T_{1\rho}$ than the β-strand residues. Field-dependent $T_{1\rho}$ analysis indicated that the shorter $T_{1\rho}$ of G10 results from larger motional amplitudes of the β-turn and not to rate differences from the rest of the peptide [26].

Molecular dynamics simulations of the S4 helix of the voltage-gated potassium channel KvAP [27] suggested that lipid headgroups and water stabilize Arg insertion by forming a hydrogen-bonded network. The effective lipid bilayer thickness was reduced to a remarkably small 10 Å near the inserted S4 helix so that water and phosphate groups can stabilize the Arg's in the middle of the S4 helix by hydrogen bonds [28]. Based on the comparison of the mean-square displacement of phosphate groups near the peptide with those far away from the peptide and the analysis of the survival function of water molecules in the system, it was found that both phosphate groups and water molecules are much less mobile in the vicinity of the guanidinium groups than in their respective bulk environments. In particular, the mean residence times for water molecules hydrogen-bonded to Arg_9 and Arg_{12} in the S4 helix, which are close to the bilayer surface, are much shorter than those hydrogen-bonded to Arg_{15} and Arg_{18}, which lie in the hydrophobic core of the membrane (90–300 ps versus 1000–2000 ps). This different residence time suggests that the water molecules near Arg in the hydrophobic core are less mobile than those near Arg at the membrane surface. This in turn suggests that Arg's in the hydrophobic part of the membrane are less mobile than those close to the bilayer surface. These are consistent with the different mobility observed between Arg_4 and Arg_{11} in PG-1.

In summary, we have measured the dipolar couplings, CSA's, and T_2 and $T_{1\rho}$ relaxation times of key Arg residues in PG-1 in the bacteria-mimetic anionic POPE/POPG membrane. The linewidths and motional scaling factors show that the β-turn Arg_{11} near the membrane surface is significantly more mobile than the β-strand Arg_4 and Leu_5 in the hydrophobic part of the membrane. The different mobility is consistent with the location of the residues with respect to the membrane, the intermolecular aggregation of this peptide, and the strong Arg-phosphate interaction. Thus, the site-specific dynamics of PG-1 correlate well with its topological and oligomeric structure. Solid-state NMR is shown to be a useful tool for elucidating the relation between membrane protein dynamics and its structure.

Experimental section

1-palmitoyl-2-oleoyl-*sn*-glycero-3-phosphatidylethanolamine (POPE), and 1-palmitoyl-2-oleoyl-*sn*-glycero-3-phosphatidylglycerol (POPG) were purchased from Avanti Polar Lipids (Alabaster, AL). PG-1 (NH_2-RGGRLCYCRRRFCVCVGR-$CONH_2$) was synthesized using Fmoc chemistry as previously described [7]. Three PG-1 samples were synthesized, containing U-^{13}C, ^{15}N-Arg_4 and ^{15}N-Leu_5, U-^{13}C, ^{15}N-Arg_{11} and ^{15}N-Phe_{12}, U-^{13}C, ^{15}N-Leu_5. U-^{13}C, ^{15}N-labeled Arg was obtained from Spectra Stable Isotopes (Columbia, MD) as Fmoc-Arg(MTR)-OH.

POPE and POPG lipids (3:1) were mixed in chloroform and blown dry under N_2 gas. The mixture was then redissolved in cyclohexane and lyophilized. The dry lipid powder was dissolved in water and subjected to five cycles of freeze-thawing to form uniform vesicles. An appropriate amount of PG-1 to reach a peptide-lipid molar ratio (P/L) of 1 : 12.5 was dissolved in water and mixed with the lipid vesicle solution, incubated at 303 K overnight, then centrifuged at 55,000 rpm for 2.5 hours. The pellet was packed into a MAS rotor, giving a fully hydrated membrane sample.

NMR experiments were carried out on a Bruker DSX-400 (9.4 Tesla) spectrometer (Karlsruhe, Germany). Triple-resonance magic-angle spinning (MAS) probes with a 4 mm

spinning module was used. Temperatures were controlled by a Kinetics Thermal Systems XR air-jet sample cooler (Stone Ridge, NY) on the 400 MHz system. Typical 90° pulse lengths were 5 – 6 μs for ^{13}C and ^{15}N, and ^{1}H decoupling fields of 50–80 kHz were used. ^{13}C chemical shifts were referenced externally to the α-Gly $^{13}C'$ signal at 176.49 ppm on the TMS scale. ^{15}N chemical shifts were referenced externally to the *N*-acetyl-Val $^{15}N\alpha$ signal at 121.72 ppm.

^{13}C-^{1}H and ^{15}N-^{1}H dipolar couplings were measured using the 2D DIPSHIFT experiment [29] at 3.0–3.5 kHz MAS with MREV-8 for ^{1}H homonuclear decoupling. Pulse lengths of 3.5 μs were used in the MREV-8 pulse train. The N-H DIPSHIFT experiments were performed with dipolar doubling [30,31] to increase the precision of the measured couplings. Some ^{13}C sites overlap with lipid peaks, so the double-quantum-filtered (DQ) DIPSHIFT experiments [1] were used to measure these dipolar couplings. The DQ filter used SPC5 homonuclear dipolar recoupling sequence [32]. The ^{13}C CSA was measured using the 2D SUPER experiment [22] under 3.5 kHz MAS. The corresponding ^{13}C field strength was 42 kHz. ^{1}H rotating-frame spin-lattice relaxation times ($T_{1\rho}$) was measured using spin-lock field strengths of 50–62.5 kHz. The ^{13}C and ^{15}N 1D spectra were measured between 243 and 308 K. All DIPSHIFT, SUPER and $T_{1\rho}$ experiments were carried out at 283 K.

Supplementary Material

Refer to Web version on PubMed Central for supplementary material.

Acknowledgments

This work is supported by the National Institutes of Health grant GM-066976 to M. H.

References

1. Huster D, Xiao LS, Hong M. Biochemistry. 2001; 40:7662–7674. [PubMed: 11412120]
2. Reuther G, Tan KT, Vogel A, Nowak C, Arnold K, Kuhlmann J, Waldmann H, Huster D. J. Am. Chem. Soc. 2006; 128:13840–13846. [PubMed: 17044712]
3. Williams JC, McDermott AE. Biochemistry. 1995; 34:8309–8319. [PubMed: 7599123]
4. Etzkorn M, Martell S, Andronesi OC, Seidel K, Engelhard M, Baldus M. Angew. Chem. Int. Ed. 2007; 46:459–462.
5. Cady SD, Goodman C, DeGrado WF, Hong M. J. Am. Chem. Soc. 2007; 129:5719–5729. [PubMed: 17417850]
6. Park SH, Mrse AA, Nevzorov AA, De Angelis AA, Opella SJ. J. Magn. Reson. 2006; 178:162–165. [PubMed: 16213759]
7. Yamaguchi S, Hong T, Waring A, Lehrer RI, Hong M. Biochemistry. 2002; 41:9852–9862. [PubMed: 12146951]
8. Bellm L, Lehrer RI, Ganz T. Exp. Opin. Invest. Drugs. 2000; 9:1731–1742.
9. Kokryakov VN, Harwig SS, Panyutich EA, Shevchenko AA, Aleshina GM, Shamova OV, Korneva HA, Lehrer RI. FEBS Lett. 1993; 327:231–236. [PubMed: 8335113]
10. Mangoni ME, Aumelas A, Charnet P, Roumestand C, Chiche L, Despaux E, Grassy G, Calas B, Chavanieu A. FEBS Lett. 1996; 383:93–98. [PubMed: 8612801]
11. Sokolov Y, Mirzabekov T, Martin DW, Lehrer RI, Kagan BL. Biochim. Biophys. Acta. 1999; 1420:23–29. [PubMed: 10446287]
12. Mani R, Cady SD, Tang M, Waring AJ, Lehrer RI, Hong M. Proc. Natl. Acad. Sci. U.S.A. 2006; 103:16242–16247. [PubMed: 17060626]
13. Tang M, Waring AJ, Hong M. J. Am. Chem. Soc. 2007; 129:11438–11446. [PubMed: 17705480]
14. Lorieau J, McDermott AE. Magn. Reson. Chem. 2006; 44:334–347. [PubMed: 16477680]

15. Lorieau JL, McDermott AE. J. Am. Chem. Soc. 2006; 128:11505–11512. [PubMed: 16939274]
16. Wylie BJ, Franks WT, Graesser DT, Rienstra CM. J. Am. Chem. Soc. 2005; 127:11946–11947. [PubMed: 16117526]
17. Hancock RE, Lehrer R. Trends Biotechnol. 1998; 16:82–88. [PubMed: 9487736]
18. Vives E, Brodin P, Lebleu B. J. Biol. Chem. 1997; 272:16010–16017. [PubMed: 9188504]
19. Jarver P, Langel U. Biochim. Biophys. Acta. 2006; 1758:260–263. [PubMed: 16574060]
20. Long SB, Campbell EB, Mackinnon R. Science. 2005; 309:897–903. [PubMed: 16002581]
21. Hong M, Griffin RG. J. Am. Chem. Soc. 1998; 120:7113–7114.
22. Liu SF, Mao JD, Schmidt-Rohr K. J. Magn. Reson. 2002; 155:15–28. [PubMed: 11945029]
23. Buffy JJ, Waring AJ, Lehrer RI, Hong M. Biochemistry. 2003; 42:13725–13734. [PubMed: 14622019]
24. Mani R, Tang M, Wu X, Buffy JJ, Waring AJ, Sherman MA, Hong M. Biochemistry. 2006; 45:8341–8349. [PubMed: 16819833]
25. Chen J, Falla TJ, Liu HJ, Hurst MA, Fujii CA, Mosca DA, Embree JR, Loury DJ, Radel PA, Chang CC, Gu L, Fiddes JC. Biopolymers. 2000; 55:88–98. [PubMed: 10931444]
26. Doherty T, Waring AJ, Hong M. Biochemistry. 2008; 47:1105–1116. [PubMed: 18163648]
27. Hessa T, White SH, von Heijne G. Science. 2005; 307:1427. [PubMed: 15681341]
28. Freites JA, Tobias DJ, von Heijne G, White SH. Proc. Natl. Acad. Sci. U. S. A. 2005; 102:15059–15064. [PubMed: 16217012]
29. Munowitz MG, Griffin RG, Bodenhausen G, Huang TH. J. Am. Chem. Soc. 1981; 103:2529–2533.
30. Hong M, Gross JD, Rienstra CM, Griffin RG, Kumashiro KK, Schmidt-Rohr K. J. Magn. Reson. 1997; 129:85–92. [PubMed: 9405219]
31. Huster D, Yamaguchi S, Hong M. J. Am. Chem. Soc. 2000; 122:11320–11327.
32. Hohwy M, Rienstra CM, Jaroniec CP, Griffin RG. J. Chem. Phys. 1999; 110:7983–7992.

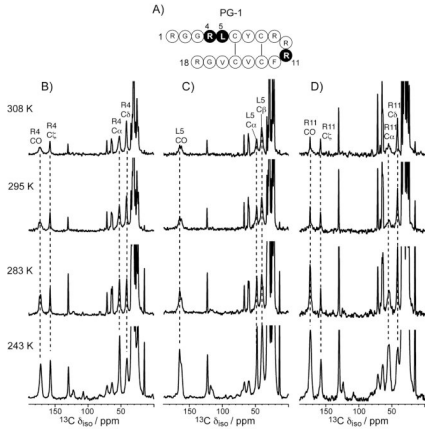

Figure 1.

^{13}C CP-MAS spectra in PG-1 bound to the POPE/POPG membrane (P/L = 1:12.5) from 243 K to 308 K. A) Amino acid sequence of PG-1. Labeled residues are shaded. B) ^{13}C CP-MAS spectra of Arg_4, C) ^{13}C CP-MAS spectra of Leu_5, D) ^{13}C CP-MAS spectra of Arg_{11}. Peptide peaks are assigned and annotated.

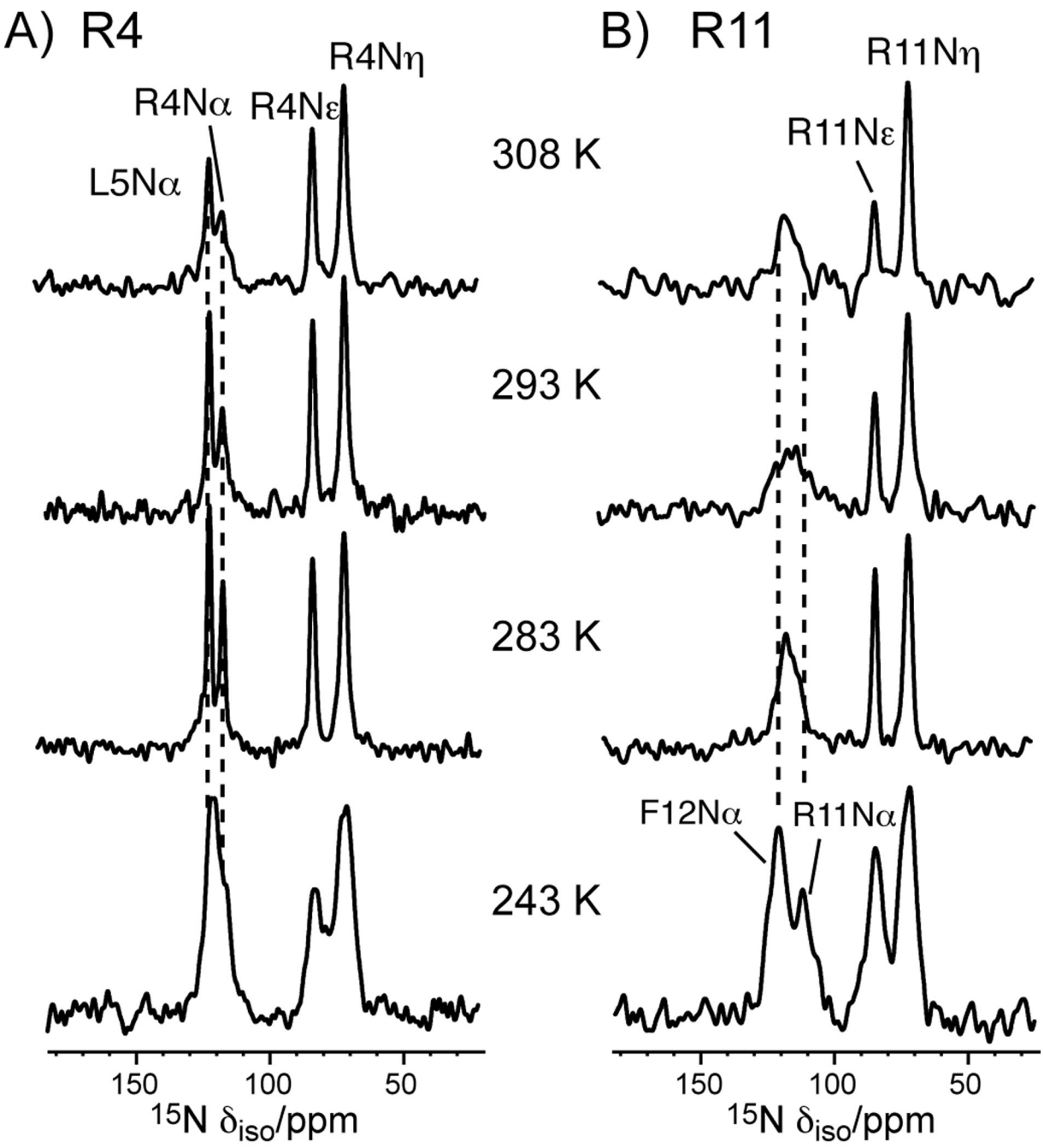

Figure 2.

^{15}N CP-MAS spectra of PG-1 in the POPE/POPG membrane at various temperatures. A) Arg_4, Leu_5. B) Arg_{11} and Phe_{12}. Assignments were obtained from ^{13}C-^{15}N 2D correlation spectra (not shown).

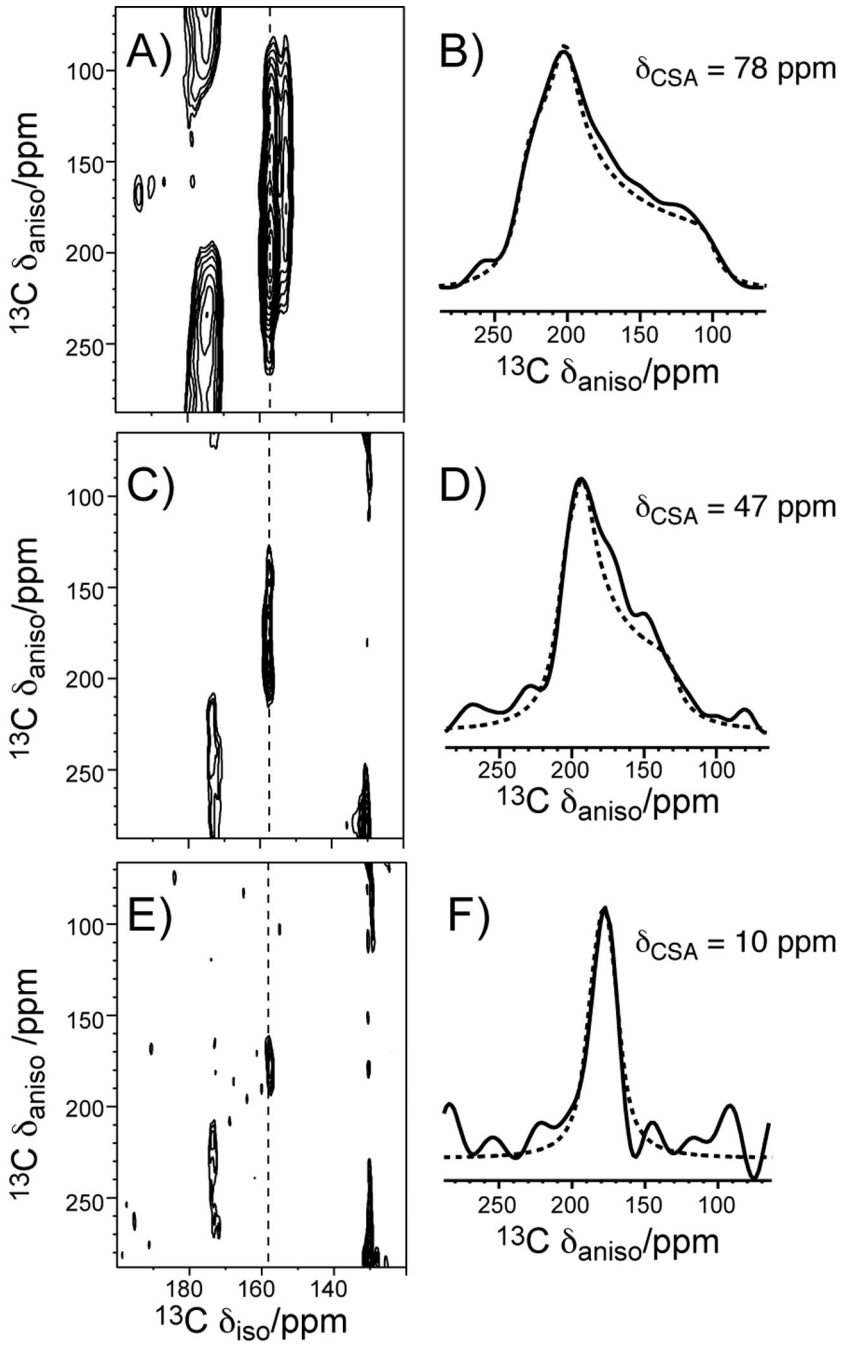

Figure 3.

Arg Cζ chemical shift anisotropies from the SUPER experiment. The 2D SUPER spectra are shown in A), C), E) and the corresponding Cζ 1D cross sections are shown in B), D), F). A, B) Fmoc-Arg(MTR)-OH. C, D) PG-1 Arg_4. E, F) PG-1 Arg_{11}. The PG-1 data were measured at 283 K in the POPE/POPG membrane.

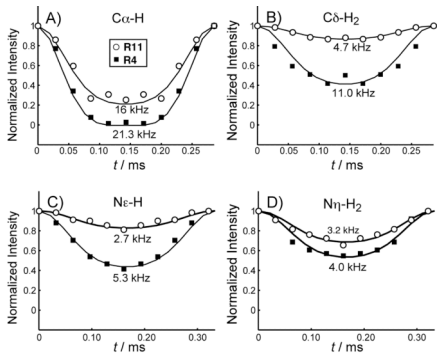

Figure 4.

^{13}C-^{1}H and ^{15}N-^{1}H DIPSHIFT curves of several sites of Arg_4 (closed squares) and Arg_{11} (open circles) in PG-1 at 283 K. A) Cα-H. B) Cδ-H_2. C) Nε-H. D) Nη-H_2. Arg_{11} gives weaker couplings than Arg_4, indicating larger motional amplitudes.

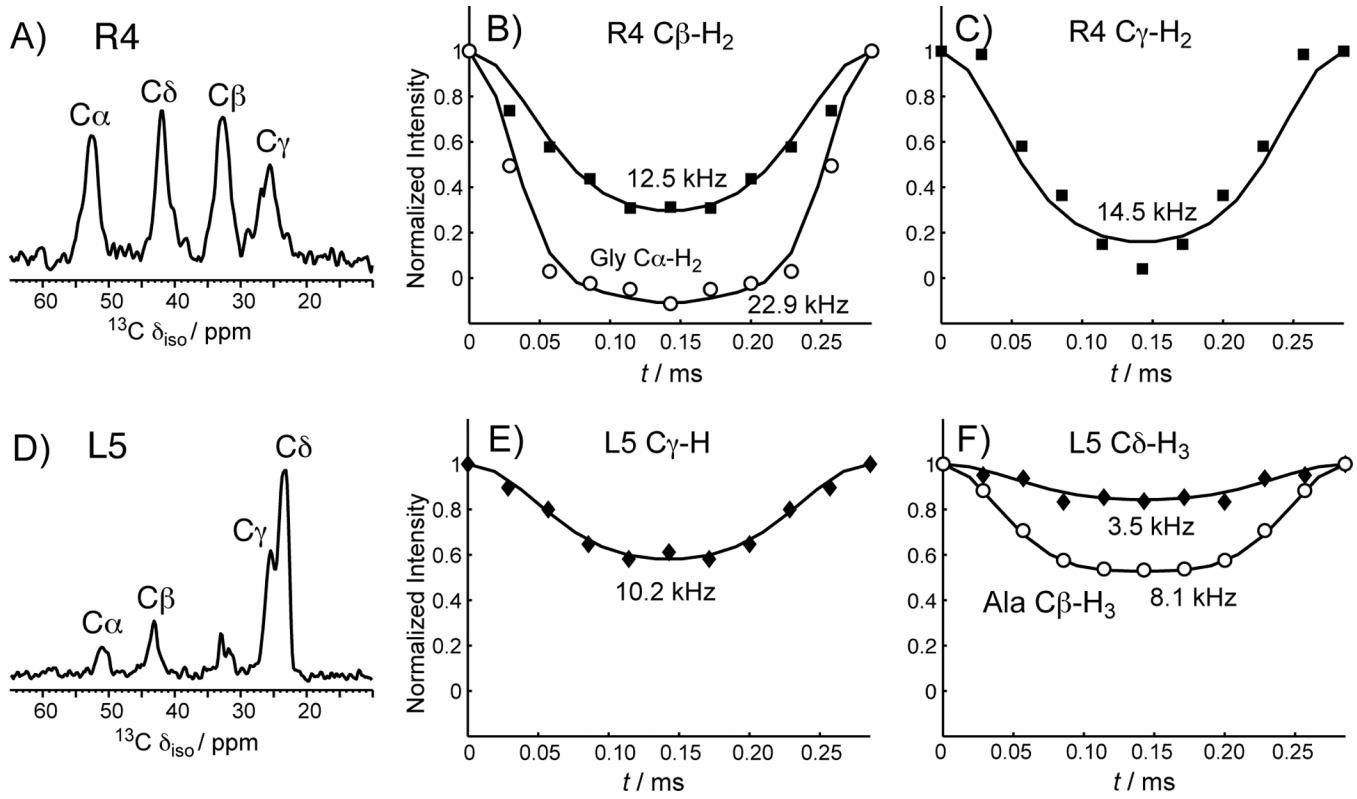

Figure 5.

1D ^{13}C DQ filtered spectra and DQ-DIPSHIFT curves of Arg_4 and Leu_5 in PG-1 in the POPE/POPG membrane. A) 1D DQ spectrum of Arg_4. The Cβ and Cγ peaks no longer overlap with the lipid peaks. B) DIPSHIFT curves of Arg_4 Cβ (squares) and the crystalline amino acid Gly Cα (circles). The Gly Cα data give the rigid-limit coupling for CH_2 groups, which is 22.9 kHz. C) DIPSHIFT curve of Arg_4 Cγ. D) 1D DQ spectrum of Leu_5. The Cγ and Cδ peaks no longer overlap with the lipid peaks. E) DIPSHIFT curve of Leu_5 Cγ. F) DIPSHIFT curves of Leu_5 Cδ (diamonds) and the crystalline amino acid Ala Cβ (circles). The Ala Cβ data give the rigid-limit coupling for methyl groups, which is 8.1 kHz. This is one-third of the one bond C-H coupling due to the three-site jump of the CH_3 group.

Table 1

^{13}C apparent linewidths (Δ*) and homogeneous linewidths (Δ) of PG-1 in POPE/POPG membrane at 283 K and 243 K. The apparent linewidths are read off from 1D CP spectra. The homogeneous linewidths are obtained from T_2 measurements as $\Delta = 1/\pi T_2$. The linewidths were measured at a ^{13}C Larmor frequency of 100 MHz.

Residue	Sites	283 K		243 K	
		Δ* / Hz	Δ / Hz	Δ * / Hz	Δ / Hz
Arg_4	Cα	272	199	222	118
	Cδ	222	187	493	289
	Cζ	111	84	201	80
Arg_{11}	Cα	473	289	604	133
	Cδ	161	106	534	265
	Cζ	81	53	222	94

Table 2

Dipolar order parameters and CSA motional scaling factors [a] of PG-1 residues at 283 K and of three crystalline model compounds at 295 K.

Sites	Arg_4	Arg_{11}	Fmoc-Arg	Arg-HCl	Leu_5	Leu
Nα	1.05	0.70	-	-	0.95	-
Cα	0.93	0.70	0.91	0.91	0.93	0.95
Cβ	0.61	-	0.86	0.91	0.56	0.93
Cγ	0.63	-	0.91	0.91	0.44	-
Cδ	0.48	0.21	0.91	1.02	0.43	0.34
Nε	0.48	0.24	-	-	-	-
$C\zeta^a$	0.61	0.13	-	-	-	-
Nη	0.36	0.28	-	-	-	-

Table 3

^{1}H $T_{1\rho}$ (ms) of POPE/POPG-bound PG-1 at 283 K and of crystalline Arg·HCl at 295 K. Experimental uncertainties are given in the parentheses. The ^{1}H spin-lock field strengths were 50 kHz in the ^{15}N-detected experiment and 62.5 kHz in the ^{13}C-detected experiments.

Sites	Arg_4	Arg_{11}	Arg · HCl
H^N	2.6 (0.2)	2.2 (0.3)	-
Hα	2.0 (0.1)	0.8 (0.1)	8.8
Hδ	1.6 (0.1)	1.9 (0.1)	9.5
Hε	2.2 (0.2)	2.6 (0.2)	8.8
Hη	1.9 (0.2)	1.8 (0.1)	8.8